PHYSICAL REVIEW C **93**, 011306(R) (2016)

α-decay width of ^{212}Po from a quartetting wave function approach

Chang Xu,[1,*] Zhongzhou Ren,[1,2,†] G. Röpke,[3,‡] P. Schuck,[4,5,§] Y. Funaki,[6] H. Horiuchi,[7,8] A. Tohsaki,[7] T. Yamada,[9] and Bo Zhou[10]

[1]*Department of Physics and Key Laboratory of Modern Acoustics, Nanjing University, Nanjing 210093, China*
[2]*Center of Theoretical Nuclear Physics, National Laboratory of Heavy-Ion Accelerator, Lanzhou 730000, China*
[3]*Institut für Physik, Universität Rostock, D-18051 Rostock, Germany and National Research Nuclear University (MEPhI), 115409 Moscow, Russia*
[4]*Institut de Physique Nucléaire, Université Paris-Sud, IN2P3-CNRS, UMR 8608, F-91406 Orsay, France*
[5]*Laboratoire de Physique et Modélisation des Milieux Condensés, CNRS- UMR 5493, F-38042 Grenoble Cedex 9, France*
[6]*RIKEN Nishina Center, Wako 351-0198, Japan*
[7]*Research Center for Nuclear Physics (RCNP), Osaka University, Osaka 567-0047, Japan*
[8]*International Institute for Advanced Studies, Kizugawa 619-0225, Japan*
[9]*Laboratory of Physics, Kanto Gakuin University, Yokohama 236-8501, Japan*
[10]*Faculty of Science, Hokkaido University, Sapporo 060-0810, Japan*

(Received 21 November 2015; revised manuscript received 18 December 2015; published 26 January 2016)

A microscopic calculation of α-cluster preformation probability and α-decay width in the typical α emitter ^{212}Po is presented. Results are obtained by improving a recent approach to describe α preformation in ^{212}Po [Phys. Rev. C **90**, 034304 (2014)] implementing four-nucleon correlations (quartetting). Using the actually measured density distribution of the ^{208}Pb core, the calculated α-decay width of ^{212}Po agrees fairly well with the measured one.

DOI: 10.1103/PhysRevC.93.011306

Radioactive α decay is a frequent phenomenon in nuclear physics, in particular near the doubly magic nuclei ^{100}Sn and ^{208}Pb and the superheavies where α decay competes with spontaneous fission (for a recent discussion see [1] and references given there). Whereas the tunneling of an α particle across the Coulomb barrier is well described in quantum physics, the problem in understanding α decay within a microscopic approach is the preformation of the α cluster in the decaying nucleus.

The formation of α-like correlations in nuclear systems has been investigated recently. In particular, in light, low density states of self-conjugate nuclei, four-nucleon correlations have been identified within the THSR (Tohsaki-Horiuchi-Schuck-Röpke) approach [2], but also with other theories such as the resonating group method [3], the generator coordinate method [4], fermion molecular dynamics [5], and antisymmetrized molecular dynamics approaches [6] going beyond the mean-field approximation. The main message is that well-defined clusters are formed only in regions where the density of nuclear matter is low. Therefore, it is of interest to investigate α-like correlations also in the outer tails of the density of a nucleus, and α preformation is discussed as a surface effect confined to the region where the nucleon density is comparable to or below 1/5 of saturation density $n_{\rm sat} = 0.16$ fm^{-3}.

A typical example is ^{212}Po, which is an α emitter with half-life 0.299 μs and decay energy $Q_\alpha = 8954.13$ keV. It is spherical, doubly magic, and has only one decay channel. Several approaches have been made to calculate the α decay width of ^{212}Po within a microscopic approach; see Ref. [7] and references therein. Furthermore a quartetting wave function approach has been worked out recently [8]. Here, we are interested in the α decay width of ^{212}Po. The transition probability for the α decay $W = P_\alpha \nu \mathcal{T}$ is given as product of the preformation probability P_α, the frequency (pre-exponential factor) ν, and the exponential factor $\mathcal{T}$. In the present work, we improve the exploratory calculation performed in [8], replacing simple expressions for the density of the ^{208}Pb core by recently measured density profiles [9]. Furthermore, we improve the mean-field potential using a double-folding potential [10] instead of the Woods-Saxon potential. To evaluate the α-decay width, we use the approach of Gurvitz [11] to estimate the pre-exponential factor. In addition to the preformation factor and the binding energy, results for the half-life will be given.

Preformation probability. An effective α-particle equation has been derived recently [8] for cases where an α particle is bound to a doubly magic core, ^{208}Pb. Neglecting recoil effects, we assume that the core nucleus is fixed at $\mathbf{r} = 0$. The core nucleons are distributed with baryon density $n_B(r)$ and produce a mean field $V_\tau^{\rm mf}(r)$ acting on the two neutrons ($\tau = n$) and two protons ($\tau = p$) moving on top of the lead core. In the present work, we will consider both $n_B(r)$ and $V_\tau^{\rm mf}(r)$ as phenomenological inputs. Of interest is the wave function of the four nucleons on top of the core nucleus, which can form an α-like cluster.

The four-nucleon wave function (quartetting state) $\Psi(\mathbf{R},\mathbf{s}_j) = \varphi^{\rm intr}(\mathbf{s}_j,\mathbf{R})\,\Phi(\mathbf{R})$ is subdivided in a unique way in the (normalized) center-of-mass (c.m.) part $\Phi(\mathbf{R})$ depending only on the c.m. coordinate $\mathbf{R}$, and the intrinsic part $\varphi^{\rm intr}(\mathbf{s}_j,\mathbf{R})$ which depends, in addition, on the relative coordinates $\mathbf{s}_j$ (for

*cxu@nju.edu.cn
†zren@nju.edu.cn
‡gerd.roepke@uni-rostock.de
§schuck@ipno.in2p3.fr

instance, Jacobi-Moshinsky coordinates) [8]. The respective c.m. and intrinsic Schrödinger equations are coupled by contributions containing the expression $\nabla_R \varphi^{\rm intr}(\mathbf{s}_j, \mathbf{R})$ which will be neglected in the present work.

The intrinsic wave equation describes in the zero-density limit the formation of an α particle with binding energy $B_\alpha = 28.3$ MeV. For homogeneous matter, the binding energy will be reduced because of Pauli blocking. In the zero-temperature case considered here, the shift of the binding energy is determined by the baryon density $n_B = n_n + n_p$, i.e., the sum of the neutron density n_n and the proton density n_p. Furthermore, Pauli blocking depends on the asymmetry given by the proton fraction n_p/n_B and the c.m. momentum $\mathbf{P}$ of the α particle. Neglecting the weak dependence on the asymmetry, for $\mathbf{P} = 0$ the density dependence of the Pauli blocking term $W^{\rm Pauli}(n_B) = 4515.9\, n_B - 100935\, n_B^2 + 1202538\, n_B^3$ was found in [8], Eq. (45), as a formula with fitted parameters valid in the density region $n_B \leqslant 0.03$ fm^{-3} with relative error below 1%. In particular, the bound state is dissolved and merges with the continuum of scattering states at the Mott density $n_B^{\rm Mott} = 0.02917$ fm^{-3}.

The intrinsic wave function remains nearly α-particle-like up to the Mott density, but becomes a product of free nucleon wave functions (more precisely the product of scattering states) above the Mott density. This behavior of the intrinsic wave function will be used below when the preformation probability for the α particle is calculated. Below the Mott density the intrinsic part of the quartetting wave function has a large overlap with the intrinsic wave function of the free α particle. In the region where the α-like cluster penetrates the core nucleus, the intrinsic bound state wave function transforms at the critical density $n_B^{\rm Mott}$ into an unbound four-nucleon shell model state. In the case of ^{212}Po considered here, an α particle is moving on top of the doubly magic ^{208}Pb core. The tail of the density distribution of the Pb core where the baryon density is below the Mott density $n_B^{\rm Mott}$ is relevant for the formation of α-like four-nucleon correlations [12]. Simply stated, the α particle can exist only at the surface of the heavy nucleus. This peculiarity has been considered for a long time for the qualitative discussion of the preformation of α particles in heavy nuclei [1,13,14].

Improving simple estimations for the baryon density considered in [8], we use the empirical results obtained recently [9] which are parametrized by Fermi functions. With the neutron density $n_n(r) = 0.093776/\{1 + \exp[(r - 6.7\ \text{fm})/0.55\ \text{fm}]\}$ fm^{-3} and the proton density $n_p(r) = 0.062895/\{1 + \exp[(r - 6.68\ \text{fm})/0.447\ \text{fm}]\}$ fm^{-3}, the Mott density $n_B^{\rm Mott} = 0.02917$ fm^{-3} occurs at $r_{\rm cluster} = 7.4383$ fm, $n_B(r_{\rm cluster}) = n_B^{\rm Mott}$. This means that α-like clusters can exist only at distances $r > r_{\rm cluster}$; for smaller values of r the intrinsic wave function is characterized by the uncorrelated motion.

Our main attention is focused on the c.m. motion $\Phi(\mathbf{R})$ of the four-nucleon wave function (quartetting state of four nucleons $n_\uparrow, n_\downarrow, p_\uparrow, p_\downarrow$). We replace the c.m. coordinate $\mathbf{R}$ by the distance r from the center of the heavy ^{208}Pb core. The corresponding Schrödinger equation contains the kinetic part $-\hbar^2\nabla^2/8m$ as well as the potential part $W(\mathbf{r}, \mathbf{r}')$, which is in general nonlocal but can be approximated by a local

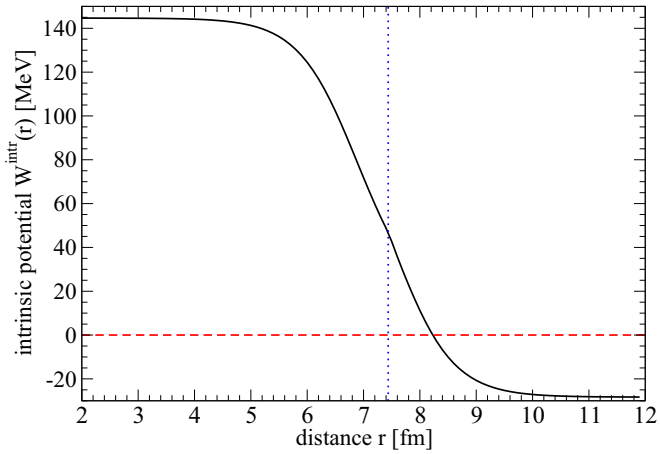

FIG. 1. Intrinsic part $W^{\rm intr}(r)$ of the effective c.m. potential $W(r)$. The empirical density distribution [9] for the ^{208}Pb core has been used. The critical radius $r_{\rm cluster} = 7.4383$ fm where the bound state are dissolved is indicated (dotted line). The four-nucleon Fermi energy $E_{4,\rm cont}(r)$ for $r < r_{\rm cluster}$ is taken in Thomas–Fermi approximation (free fermion gas).

effective c.m. potential $W(r) = W^{\rm intr}(r) + W^{\rm ext}(r)$. The effective c.m. potential consists of two contributions: the intrinsic part $W^{\rm intr}(r) = E_\alpha^{(0)} + W^{\rm Pauli}(r)$ and the external part $W^{\rm ext}(r)$ which is determined by the mean-field interaction $V_\tau^{\rm mf}(r)$ [8].

The intrinsic part $W^{\rm intr}(r)$ approaches for large r the bound state energy $E_\alpha^{(0)} = -B_\alpha = -28.3$ MeV of the α particle. In addition, it contains the Pauli blocking effects $W^{\rm Pauli}[n_B(r)]$ given above [8], which leads for $r > r_{\rm cluster}$ to a shift of the binding energy of the α-like cluster. For $r < r_{\rm cluster}$, the density of the core nucleus is larger than the Mott density so that no bound state is formed. As lowest energy state, the four nucleons of the quartetting state are added at the edge of the continuum states $E_{4,\rm cont}$. In the case of the Thomas-Fermi model, not accounting for an external potential, the edge of the four-nucleon continuum coincides with the sum of the Fermi energies of the four nucleons, $E_{4,\rm cont} = 2E_{{\rm F},n}(n_n) + 2E_{{\rm F},p}(n_p)$ with $E_{{\rm F},\tau}(n_\tau) = (\hbar^2/2m_\tau)(3\pi^2 n_\tau)^{2/3}$. Because the nucleon densities $n_\tau(r)$ depend on position r, also the continuum edge of unoccupied states $E_{4,\rm cont}(r)$ will depend on r. For illustration, the intrinsic part $W^{\rm intr}(r)$, based on the empirical density distribution [9] for the ^{208}Pb core, is shown in Fig. 1.

The external part $W^{\rm ext}(\mathbf{r})$ is given by the mean field $V_\tau^{\rm mf}(r)$ of the surrounding matter acting on the four-nucleon system. It includes the strong nucleon-nucleon interaction as well as the Coulomb interaction. For $r > r_{\rm cluster}$ the simple Woods-Saxon potential used in [8] can be improved by using the double-folding potential [15], which contains the direct nucleon-nucleon interaction and the exchange terms. The Coulomb interaction is calculated as a double-folding potential using the proton density $n_p(r)$ of the ^{208}Pb core given above and a Gaussian density distribution for the α cluster, with a charge r.m.s. radius of 1.67 fm. The direct nucleon-nucleon interaction is obtained by folding the measured nucleon density distribution of the ^{208}Pb core $n_B(r)$ and the Gaussian density distribution for the α cluster (point r.m.s. radius 1.44 fm) with a parameterized M3Y-type nucleon-nucleon effective interaction

$v(s) = c\exp(-4s)/(4s) - d\exp(-2.5s)/(2.5s)$ describing a short-range repulsion (c) and a long-range attraction (d); s denotes the nucleon-nucleon distance. For comparison, two sets of c.m. potentials from the double-folding procedure are discussed here: potential A and potential B. For $r > r_{\rm cluster}$, the corresponding parameter values for c,d of the direct term $V_N(r)$ are given in Table I. For the exchange terms we use the Pauli blocking $W^{\rm Pauli}[n_B(r)]$ obtained from the microscopic approach. Potential A is considered to explain the physics underlying our approach. The core nucleus is treated in the Thomas-Fermi approximation. Potential B takes into account a discrete level structure in the core nucleus.

Potential A: Thomas-Fermi model for the core region. The Thomas-Fermi model of the core nucleus considers a (self-consistent) mean-field potential $V_\tau^{\rm mf}(r)$. The baryon density $n_\tau(r)$ yields the Fermi energy $E_{{\rm F},\tau}(r)$ (ideal Fermi gas approximation) as given above. We can introduce the chemical potential $\mu_\tau(r) = V_\tau^{\rm mf}(r) + E_{{\rm F},\tau}(r)$ with the property that an additional baryon, introduced at position r, must have at least the energy $\mu_\tau(r)$. The well-known variational principle leads to a uniform μ_τ for the entire nucleon system, not depending on position r and determined only by the total baryon number.

The same argumentation can also applied to four nucleons in different spin-isospin states as long as they are moving in free, uncorrelated states. This is the case for the core region $r < r_{\rm cluster}$ where no bound state can be formed by the four nucleons added to the ^{208}Pb core. Here, the intrinsic wave function $\varphi^{\rm intr}(\mathbf{s}_j,\mathbf{R})$ is approximated by the antisymmetrized product of free single-nucleon states. Within a local-density (Thomas-Fermi) approach these four nucleons are added at the respective Fermi energies $E_{{\rm F},\tau}(r)$, i.e., at the chemical potential μ_4 which is the sum of the mean-field potential and the Fermi energy of the four nucleons, $\mu_4 = W^{\rm ext}(r) + E_{4,{\rm cont}}(r) = 2V_n^{\rm mf}(r) + 2V_p^{\rm mf}(r) + 2E_{{\rm F},n}(n_n(r)) + 2E_{{\rm F},p}(n_p(r))$. In the region $r < r_{\rm cluster}$ where the Thomas-Fermi approach can be applied (independent single-nucleon motion), according to the variational principle the energy value μ_4 is a constant, not depending on position r. (Note that this argumentation cannot applied to the region $r > r_{\rm cluster}$ where a bound state can be formed. Here, correlations are essential, and the use of the Thomas-Fermi approach is not possible.)

The Schrödinger equation for the c.m. motion [8], governed by the effective c.m. potential $W(R)$, determines the wave function $\Phi(\mathbf{R})$ as well as the energy eigenvalue E. This energy eigenvalue of the four-nucleon system on top of the ^{208}Pb core nucleus coincides, on the one hand, with the bound state energy $E_{\rm tunnel}$ of the four-nucleon cluster; see the discussion of the tunneling process given below. On the other hand, in the region $r < r_{\rm cluster}$ where the Thomas-Fermi approach can be applied, the ground state energy E for the four-nucleon system on top of the ^{208}Pb core was found to be μ_4 as discussed above. In conclusion, in the Thomas–Fermi approach for the core region $r < r_{\rm cluster}$, the chemical potential μ_4 coincides with the bound state energy $E_{\rm tunnel}$ of the four-nucleon cluster, $E_{\rm tunnel} = \mu_4$. In this region, the effective c.m. potential $W(r)$ describes the edge of the four-nucleon continuum where the nucleons can penetrate into the core nucleus.

Potential A is designed according to this simple local-density approach. The two parameter values $c_{\rm A}$,$d_{\rm A}$ are determined by the conditions $\mu_4 = E_{\rm tunnel} = -19.346$ MeV; see Fig. 2. The tunneling energy is identical to the energy at which the four nucleons are added to the core nucleus. The total c.m. potential is continuous at $r = r_{\rm cluster}$ and is constant for $r < r_{\rm cluster}$, where the effective c.m. potential is $W(r) = \mu_4$. The corresponding values for the preformation factor and the decay half-life are given in Table I.

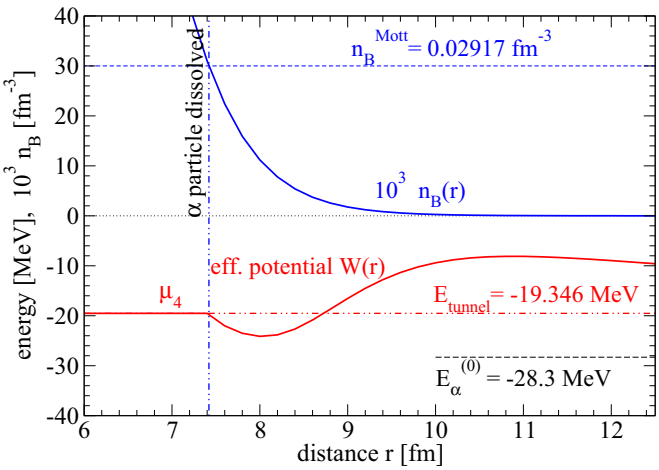

FIG. 2. Effective c.m. potential $W(r)$, potential A. The empirical baryon density distribution $n_B(r)$ [9] for the ^{208}Pb core is also shown. The chemical potential μ_4 coincides with the binding energy $E_{\rm tunnel}$.

Potential B: Discrete energy level structure of the core nucleus. In a better approximation, the simple local-density (Thomas-Fermi) approach for the ^{208}Pb core nucleus has to be replaced by a shell model calculation. Then, the single-particle states are occupied up to the Fermi energy, and additional nucleons are introduced at higher energy levels according to the discrete structure of the single energy level spectrum. The continuous energy spectrum of the Thomas-Fermi approach which prescribes that, if all states below the chemical potential μ_τ are occupied, an additional nucleon introduced in the nuclear system has the minimum energy μ_τ, is no longer valid, and the condition $E_{\rm tunnel} = \mu_4$ is withdrawn. If the shell model is appropriate for the core nucleus, with the Fermi energy at μ_4, additional nucleons have a somewhat higher energy, $E_{\rm tunnel} > \mu_4$. (Note that in the opposite case a shell model approach becomes unstable against the formation of clusters.)

Potential B is designed without the condition $\mu_4 = E_{\rm tunnel}$. The two parameter values $c_{\rm B}$,$d_{\rm B}$ are determined by the two empirical values: the bound state energy $E_{\rm tunnel} = -19.346$ MeV and the half-life $T_{1/2} = 2.99 \times 10^{-7}$ s for ^{212}Po. The corresponding values are given in Table I. As expected, the bound state energy is above the value $W(r) = \mu_4$ for the c.m. potential at $r < r_{\rm cluster}$. A plot of the c.m. potential as well as the different contributions are shown in Fig. 3. As clearly seen in Fig. 3, both the potentials A and B are dominated by the Coulomb repulsion for finite distances $r \geqslant 15$ fm, and at large distances only the bound state energy of the free α particle remains: $\lim_{r\to\infty} W(r) = -28.3$ MeV. Below $r \approx 15$ fm, both the attractive nuclear potential and repulsive Pauli blocking between the α particle and the lead core become relevant. At a critical distance $r_{\rm cluster} = 7.4383$ fm (where

TABLE I. The calculated preformation probability and decay half-life of ^{212}Po using different sets of effective c.m. potentials.

Potential	c (MeV fm)	d (MeV fm)	$E_{\rm tunnel}$ (MeV)	Fermi energy μ_4 (MeV)	$E_{\rm tunnel}-\mu_4$ (MeV)	Preform. factor P_α	Decay half-life $T_{1/2}$ (s)
A	13866.30	4090.51	−19.346	−19.346	0	0.367	2.91×10^{-8}
B	11032.08	3415.56	−19.346	−19.771	0.425	0.142	2.99×10^{-7}

$n_B = 0.02917$ fm^{-3}), the α cluster is suddenly dissolved and the four nucleons added to the core are assumed to occupy single-nucleon states above the Fermi energy μ_4.

Frequency (pre-exponential factor) ν and exponential factor $\mathcal{T}$. Using the two-potential approach of Gurvitz [11], the effective c.m. potential $W(r)$ is separated into two parts at $r_{\rm sep} = 15$ fm (the precise choice of the separating point will almost not affect the final results). By solving the corresponding c.m. Schrödinger equations, both the bound state wave function $\Phi(r)$ and the scattering state wave function $\chi(r)$ are calculated. We show both $\Phi(r)$ and $\chi(r)$ obtained from potential B in Fig. 4. The c.m. wave function $\Phi(r)$ exhibits an approximately linear increase up to the critical distance $r_{\rm cluster} = 7.4383$ fm (where $n_B = n_B^{\rm Mott}$) and then decreases. As shown in [8], the four-nucleon intrinsic wave function $\varphi^{\rm intr}(\mathbf{s}_j, r)$ is nearly identical with the free α-particle wave function in the region $r > r_{\rm cluster}$, whereas for $r < r_{\rm cluster}$ the intrinsic wave function behaves like a product of free nucleon wave functions so that the overlap with the free α-particle wave function is nearly zero. The preformation probability of the α cluster is obtained by integrating the $\Phi(r)$ from this critical point to infinity [8]:

$$P_\alpha = \int_0^\infty d^3r |\Phi(r)|^2 \Theta\left[n_B^{\rm Mott} - n_B(r)\right]. \quad (1)$$

The scattering state wave function $\chi(r)$ exhibits a strong oscillating feature as a combination of regular and irregular Coulomb functions. The decay width is then calculated by using the values of $\Phi(r)$ and $\chi_k(r)$ at the separation point. We choose $r_{\rm sep} = 15$ fm [11]:

$$\Gamma = \nu \times \mathcal{T} = \frac{4\hbar^2\alpha^2}{\mu k} |\Phi(r_{\rm sep})\chi_k(r_{\rm sep})|^2, \quad (2)$$

where $\mu = A_\alpha A_d/(A_\alpha + A_d)$, $\alpha = \sqrt{2\mu(V(r_{\rm sep}) - E_{\rm tunnel})}/\hbar$, $k = \sqrt{2\mu E_{\rm tunnel}}/\hbar$, A_d is the mass number of the lead core, and the decay half-life is related to the preformation probability and decay width by $T_{1/2} = \hbar \ln 2/(P_\alpha \Gamma)$.

Results. In Table I, the details of the calculated preformation probability and decay half-life of ^{212}Po are presented. Both potentials A and B are designed (parameter values c,d for A, B) so that the experimental bound state energy $E_{\rm tunnel} = -19.346$ MeV is reproduced. If the Thomas-Fermi condition $E_{\rm tunnel} = \mu_4$ is fixed (potential A), the calculated half-life $T_{1/2}$ is too short. The measured decay half-life $T_{1/2} = 2.99\times10^{-7}$ s is used to design potential B. The corresponding Fermi energy of potential B is $\mu_\alpha = -19.771$ MeV and the α-cluster preformation factor is $P_\alpha = 0.142$. It is emphasized that the preformation factor and decay half-life of ^{212}Po are consistently computed in a microscopic way, but the parameter values c and d of potential B were chosen to fit these empirical data.

By varying the parameters c,d of the nucleon-nucleon effective interaction $v(s)$ so that the energy eigenvalue $E_{\rm tunnel} = -19.346$ MeV (or decay energy) remains fixed, the difference $E_{\rm tunnel} - \mu_4$ changes. At the same time, the preformation

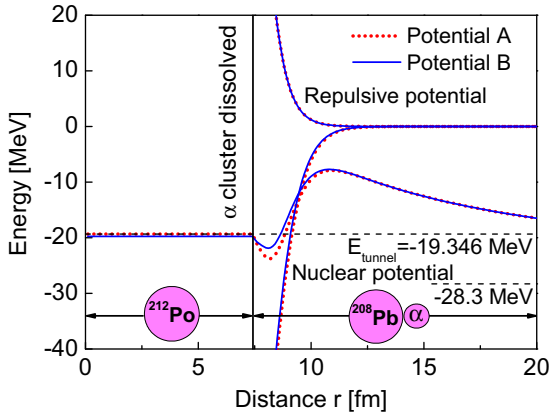

FIG. 3. Effective c.m. potential $W(r)$ for the α decay of ^{212}Po. Both versions A and B lead to the empirical bound state energy $E_{\rm tunnel} = -19.346$ MeV; see Table I. The repulsive potential is given by the Pauli blocking term. The total c.m. potential $W(r)$ contains, in addition, the Coulomb part and the bound state energy $E_\alpha^{(0)} = -28.3$ MeV. The chemical potential μ_4 for potential B is slightly deeper than the bound state energy $E_{\rm tunnel} = -19.346$ MeV; see Table I.

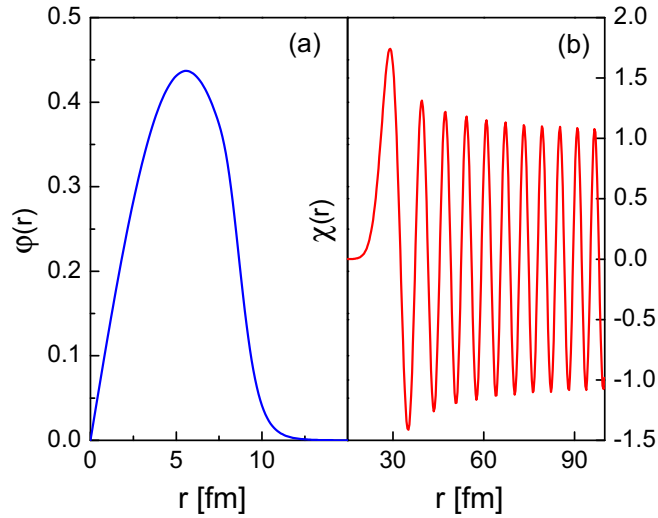

FIG. 4. The bound state wave function $\Phi(r)$ and the scattering state wave function $\chi(r)$ calculated by separating potential B into two parts based on the two-potential approach. The separation point is chosen to be $r_{\rm sep} = 15$ fm.

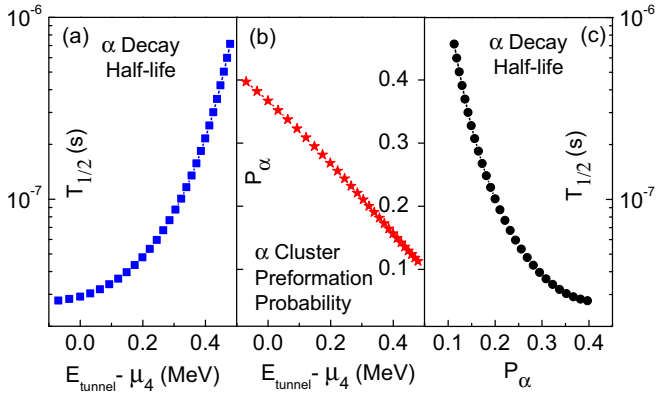

FIG. 5. Model calculations for various parametrizations c,d of the direct term $v(s)$. (a) Variation of the decay half-life with the energy difference $E_{\text{tunnel}} - \mu_4$. (b) Variation of preformation factor with the energy difference $E_{\text{tunnel}} - \mu_4$. (c) Variation of the decay half-life with the preformation factor.

factor P_α and the decay half-life $T_{1/2}$ are also changing; see also Table I for two special values. To show this behavior more clearly, the correlation between the energy difference $E_{\text{tunnel}} - \mu_4$ and the decay half-life $T_{1/2}$ is given in the left panel of Fig. 5 for various parameter values c,d of the direct term $v(s)$. Comparing potentials A and B, it is also observed that the α cluster preformation factor P_α is also correlated with the difference between the the energy eigenvalue E_{tunnel} and the Fermi energy μ_4. A systematic dependence of the preformation factor on $E_{\text{tunnel}} - \mu_4$ as well as the resulting correlation between $T_{1/2}$ and P_α at fixed decay energy is also shown in Fig. 5.

Discussion. We neglected gradient terms so that our approach is close to the local-density approximation. We have to remember that within a rigorous approach the c.m. potential $W(\mathbf{r},\mathbf{r}')$ is nonlocal. A full treatment of the inhomogeneous case relevant for finite nuclei, which includes the gradient terms and the nonlocal potentials, is a future goal, presently not in reach. In addition, an improved approach for the intrinsic wave function $\varphi^{\text{intr}}(\mathbf{s}_j;\mathbf{R})$, with a smooth behavior at r_{cluster} to replace the step function $\Theta[n_B^{\text{Mott}} - n_B(r)]$, will improve the result for P_α. The core is described by an uncorrelated quasiparticle model, the Thomas-Fermi model, or the nuclear shell model with a Fermi energy. Also pairing correlations can be introduced. It is an important task to improve the description of the core, allowing also for correlations. This would affect our understanding of the potential and the wave function for $r < r_{\text{cluster}}$ where a constant Fermi energy or chemical potential μ_4 is considered. Instead, the c.m. potential $W(r)$ and consequently the wave function $\Phi(r)$ will depend on r in a more complex way also for $r < r_{\text{cluster}}$. Presently, there are different attempts to include few-nucleon correlations to calculate light nuclei. The treatment of heavier nuclei is not feasible with present computer capabilities. The approach is inspired by the THSR wave function concept that has been successfully applied to light nuclei. Shell model calculations are improved by including four-particle (α-like) correlations that are of relevance when the matter density becomes low. A closer relation of the calculation presented here to the THSR calculations is of great interest; see the calculations for ^{20}Ne [16,17]. Related calculations are performed in Ref. [18]. A comparison with THSR calculations would lead to a better understanding of the microscopic calculations, in particular the c.m. potential, the c.m. wave function, and the preformation factor.

Acknowledgments. This work is supported by the National Natural Science Foundation of China (Grants No. 11175085, No. 11575082, No. 11535004, No. 11375086, No. 11120101005, and No. 11235001).

[1] D. S. Delion, R. J. Liotta, and R. Wyss, Phys. Rev. C **92**, 051301(R) (2015).
[2] A. Tohsaki, H. Horiuchi, P. Schuck, and G. Röpke, Phys. Rev. Lett. **87**, 192501 (2001).
[3] J. A. Wheeler, Phys. Rev. **52**, 1083 (1937).
[4] D. L. Hill and J. A. Wheeler, Phys. Rev. **89**, 1102 (1953).
[5] M. Chernykh, H. Feldmeier, T. Neff, P. von Neumann-Cosel, and A. Richter, Phys. Rev. Lett. **98**, 032501 (2007), and refs. therein.
[6] Y. Kanada-En'yo, Progr. Theor. Phys. **117**, 655 (2007), and refs. therein.
[7] K. Varga, R. G. Lovas, and R. J. Liotta, Phys. Rev. Lett. **69**, 37 (1992).
[8] G. Röpke, P. Schuck, Y. Funaki, H. Horiuchi, Z. Ren, A. Tohsaki, C. Xu, T. Yamada, and B. Zhou, Phys. Rev. C **90**, 034304 (2014).
[9] C. M. Tarbert *et al.*, Phys. Rev. Lett. **112**, 242502 (2014).
[10] S. Misicu and H. Esbensen, Phys. Rev. C **75**, 034606 (2007); **76**, 054609 (2007).
[11] S. A. Gurvitz, Phys. Rev. A **38**, 1747 (1988); S. A. Gurvitz and G. Kalbermann, Phys. Rev. Lett. **59**, 262 (1987).
[12] S. Typel, Phys. Rev. C **89**, 064321 (2014).
[13] Y. Ren and Z. Ren, Phys. Rev. C **85**, 044608 (2012); C. Xu and Z. Ren, *ibid.* **74**, 014304 (2006).
[14] V. Yu. Denisov and A. A. Khudenko, Phys. Rev. C **79**, 054614 (2009).
[15] G. R. Satchler and W. G. Love, Phys. Rep. **55**, 183 (1979).
[16] B. Zhou, Z. Ren, C. Xu, Y. Funaki, T. Yamada, A. Tohsaki, H. Horiuchi, P. Schuck, and G. Röpke, Phys. Rev. C **86**, 014301 (2012).
[17] B. Zhou, Y. Funaki, H. Horiuchi, Z. Ren, G. Röpke, P. Schuck, A. Tohsaki, C. Xu, and T. Yamada, Phys. Rev. C **89**, 034319 (2014).
[18] W. Horiuchi and Y. Suzuki, Phys. Rev. C **89**, 011304(R) (2014).